Robotica (2009) volume 27, pp. 511–528. © 2008 Cambridge University Press
doi:10.1017/S0263574708004906 Printed in the United Kingdom

The effects of parameter variation on the gaits of passive walking models: simulations and experiments

Liu Ning, Li Junfeng and Wang Tianshu*

School of Aerospace, Tsinghua University, Beijing, China

(Received in Final Form: July 3, 2008. First published online: August 14, 2008)

SUMMARY

We have made a systematic study of the gait of a straight leg planar passive walking model through simulations and experiments. Three normalised parameters, which represent the foot radius, the position of the mass centre and the moment of inertia, are used to characterise the walking model.

In the simulation, we have obtained the fixed points and the basins of attraction of the walking models with different parameter combinations by the aid of the cell mapping method. With the results of fixed points, we investigated the effects of parameter variations on the gait descriptors, including step length, period, average speed and energy inefficiency. A model that has a large basin of attraction has been obtained, and it can start walking far from its fixed point. However, the size of the basin of attraction is not a good measurement of robustness. Thus, we proposed floors with random slope angles or stairs with random heights to test robustness. Five hundred times of simulations with 100 non-dimensional time units were implemented for each parameter combination. The times that the walker failed to arrive at the end were recorded. The simulation results showed that the model with a larger foot radius and higher position of mass centre has a lower possibility of falling on uneven floors. A large moment of inertia is helpful for walking on a random slope angle floor, while low values of moment of inertia are good for navigating random stairs.

Prototype experiments have validated the simulation results, which showed that models with larger feet have a longer step length and high speed. However, period differences were difficult to obtain in the experiments since the differences were very small. We have tested the sensitivity with the initial conditions of the models with different foot radii on a flat floor, and have also tested the robustness of the models on a floor with random slope angles. The times that the model reached the end of the floor were recorded. The experimental results showed that a large foot radius is good for improving the basin of attraction and robustness on uneven floors. Finally, the exceptions of the experiment are explained.

KEYWORDS: Passive dynamic walking; Cell mapping method; Random perturbation; Experiment; Basins of attraction; Robustness.

* Corresponding author. E-mail: tswang@tsinghua.edu.cn

1. Introduction

Biped robots are the most attractive type of robots since they walk like humans. Many biped robots have been made, such as the prototypes developed by Honda and Sony. However, these biped robots have mechanical gaits and require great amounts of energy. Passive walking might be a solution. Pioneered by McGeer,[1] many researchers have shown that completely unactuated and uncontrolled machines could walk stably downhill on a gentle slope, powered only by gravity, both in numerical simulations and physical experiments.[2–6] Moreover, some actuated prototypes have been constructed based on passive dynamics.[7–9] In contrast with their traditional cousins, biped robots based on passive walking have good energy efficiency and can perform more natural gaits. It seems that the mechanical parameters of these walkers work better than the complicated control system of the conventional robots in generating natural looking gaits.

Many types of passive dynamic walkers have been studied by researchers, from simple to complex. Garcia *et al.* concocted the simplest 2D model, which has only one free parameter, the slope angle. They studied the dynamics of this model analytically and discussed the relationship of the gait and the slope angle.[10] Goswami *et al.*[4] studied a compass-like model that has point masses at the hip and on each leg. They showed that each of the parameter, namely, the slope angle, the mass ratio and the length ratio of the biped model, affects the gait in the same qualitative manner. Garcia[3] also presented some mass distribution conditions necessary for efficient walking. Wisse *et al.*[11–13] implemented physical model experiments and validated their method for preventing falling forward, adding an upper body and compensating for the yaw and roll motion of a 3D model, and they also suggested conducting a decisive study on the effect of round feet on the basin of attraction of passive walkers.[8,13,14] Asano and Luo[15] discussed the effect of semi-circular feet on the gait, but their model was actuated, and some characteristics might be changed by control laws and actuation. Hass *et al.*[16] optimised the mass distributions to obtain the maximum speed of a straight-leg point-foot model. Limited experimental results of the effects of the parameters on the gait have been reported. Wu and Sabet[17] studied the effects of changes in the ramp angle, hip mass, friction of the ramp and foot length on the walking patterns of a 2D straight-leg flat-footed model, experimentally.

For a passive walker, most of the arbitrary initial state variables might lead to a fall. If periodical gait exists, it can be treated as a Poincaré map, and Newton–Raphson iteration is used by most researchers for searching fixed points. However, the initial values of the iteration still must be guessed, and an unlucky guess often leads to divergence.[1,3,8] If a model has a stable periodical gait, it can begin at any point of the limit cycle. Furthermore, successful walking can start from the neighbourhood of the limit cycle and the set of state variables from which the walker can walk successfully is called the basin of attraction of the cyclic motion. Schwab and Wisse have obtained the basin of attraction of the cyclic motion of the simplest model with the aid of the cell mapping method. The basin of attraction of the simplest model is very small according to an experiment in which the prototype could only endure small disturbance.[14] Many researchers have reported that passive walkers have very low tolerance for large disturbances. McGeer's[1] model can absorb a perturbation of 150% of one initial angular velocity, but at the same time, the angular velocity of the other leg can only tolerate an error of a few percent. Goswami *et al.*[4] gave an example in which the angular velocity can be more than 100 deg/s, whereas the change of angle must be limited to 2°. Their reports focused on the disturbance of the initial state variables of walking motions; however, the robustness of passive models during the whole walking is more significant.

McGeer[1] has suggested that the resistance of jostling can be used for measuring robustness. Byl and Tedrake[18] have analysed the stability of passive compass gait walkers on uneven (rough) downhill terrain. They introduced the concept of the mean first passage time (MFPT) to quantify walking stability. Su and Dingwell[19] have examined how orbital stability varies as the surface bumpiness increases, and their results showed that orbital stability is not related to the perturbation magnitude applied to the system. Currently most commonly used robustness measurement is the maximal floor height variation a walker can handle without falling. Most of the actuated biped walkers based on passive walking can deal with single step-down disturbance smaller than 5% of leg length.[20]

After a systematic study of Goswami *et al.*,[4] there is still a need for an elaborate investigation on the effect of parameter variations on the gait of a straight-leg model with round feet. Moreover, there is not much experimental work to validate the simulations. In the following sections, we first introduce our passive model briefly, and then describe the use of the cell mapping method to obtain the fixed points and the basins of attraction of models with different parameter combinations. In addition, the gaits are also described by some descriptors such as the step length, period, average speed and energy inefficiency. The effects of the parameter variations on the gait are summarised and a model that has a large basin of attraction has been obtained. We used floors with random slope angles and random stairs to test the robustness of the model and describe the robustness by the fall ratio. Experiments on models with different feet radii have validated some of our simulation results, and the exceptions in the experiment are discussed.

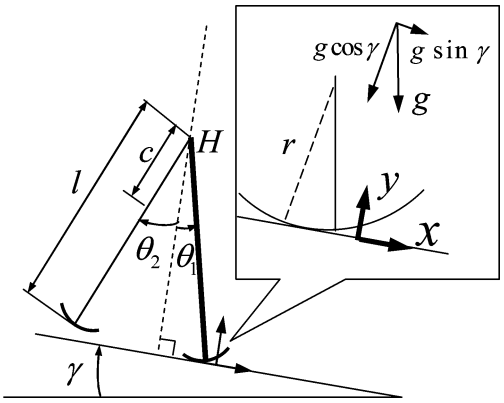

Fig. 1. Sketch of the model.

2. Modelling

Consider a planar model that consists of a pair of rigid legs with round feet, interconnected through a frictionless hinge, as shown in Fig. 1. We assume that there is no slip between the foot of the stance leg and the rigid floor. The impact between the foot of the swing leg and the floor is modelled as fully inelastic and instantaneous, which means that no slip and no bounce occur, and an exchange occurs between the stance and the swing leg at the impact time. Due to the oversimplification of the kneeless model, foot scuffing occurs at mid stance and will be neglected in the simulation.

For simplicity, the model is set to be symmetrical, and each of the legs has a mass of m, a length of l and a moment of inertia of J, including the corresponding foot. The distance between the centre of mass and the hip is c. Each foot is a part of a circle and has a radius of r. In order to reduce the number of parameters and generalize the dynamic equations, we non-dimensionalise the model by setting $k_r = r/l$, $k_c = c/l$ and $k_J = J/ml^2$, and rescale the time by $\sqrt{l/g}$. The slope angle γ is set as 0.02 rad.

We are interested in the effects of parameter variation on the gait; thus, we need to determine the parameter combinations. The interval of the non-dimensional foot radius k_r was set as [0.0, 0.5], and k_c varies from 0.1 to 0.9; both of them have the spacing of 0.1. When the centre of mass is determined, the boundary of the moment of inertia is determined but can vary independently in this interval. For example, when k_c is 0.4, k_J can be any value in the interval (0, 0.24). The values of k_J that we used in our simulation are shown in Table I.

This model has two degrees of freedom and the variables are set to be θ_1 and θ_2. The dynamic equations of the motion between heelstrike can be derived by the Lagrange equation

Table I. Values of the moment of inertia and the centre of mass.

k_c	k_J									
0.1 (0.9)	0.01	0.02	0.04	0.06	0.09	–	–	–	–	–
0.2 (0.8)	0.01	0.02	0.04	0.06	0.09	0.12	0.16	–		
0.3 (0.7)	0.01	0.02	0.04	0.06	0.09	0.12	0.16	0.21	–	–
0.4 (0.6)	0.01	0.02	0.04	0.06	0.09	0.12	0.16	0.21	0.24	–
0.5	0.01	0.02	0.04	0.06	0.09	0.12	0.16	0.21	0.24	0.25

https://doi.org/10.1017/S0263574708004906 Published online by Cambridge University Press

of the second kind in the form as follows:

$$\begin{bmatrix} M_{11} & M_{12} \\ M_{21} & M_{22} \end{bmatrix} \begin{bmatrix} \ddot{\theta}_1 \\ \ddot{\theta}_2 \end{bmatrix} = \begin{bmatrix} f_1(\theta, \dot{\theta}) \\ f_2(\theta, \dot{\theta}) \end{bmatrix} \tag{1}$$

where

$$\begin{aligned} M_{11} &= k_J + (2k_r - 1)^2 + (k_c - 1)^2 + 2k_c k_r \\ &\quad - 2k_r \cos\theta_1 (2k_r + k_c - 2), \\ M_{12} &= M_{21} = k_c[(k_r - 1)\cos(\theta_2 - \theta_1) - k_r \cos\theta_2], \\ M_{22} &= k_c^2 + k_J, \\ f_1 &= k_r \dot{\theta}_1^2 \sin\theta_1 (2 - k_c - 2k_r) + k_c \dot{\theta}_2^2 \sin(\theta_2 - \theta_1)(k_r - 1) \\ &\quad - k_c k_r \dot{\theta}_2^2 \sin\theta_2 + g \sin(\theta_1 - \gamma_i)(2 - k_c - 2k_r) \\ &\quad - 2g k_r \sin\gamma_i \text{ and} \\ f_2 &= -k_c (k_r - 1)\dot{\theta}_1^2 \sin(\theta_2 - \theta_1) - g k_c \sin(\theta_2 - \gamma_i). \end{aligned}$$

The heelstrike is regarded as a fully inelastic and instantaneous impact, which means the roles of the stance and the swing leg are exchanged at the heelstrike. Since the general coordinates are consistent with the leg numbers, the variables θ_1 and θ_2 will not change at the heelstrike but the form of Eq. (1) needs to be modified. Because the model is symmetric, the equations are modified by exchanging the θ_1 and θ_2 of Eq. (1). As mentioned earlier, the angles will not change at heelstrike. Nevertheless, the angular velocities just before collision, $\dot{\theta}_1^-$ and $\dot{\theta}_2^-$, will change to $\dot{\theta}_1^+$ and $\dot{\theta}_2^+$. These can be obtained from the conservation of angular momentum of the model about the contact point C and of the new swing leg (old stance leg) about the hinge H, as follows:

$$\begin{aligned} L_C^-(\theta_1^-, \theta_2^-, \dot{\theta}_1^-, \dot{\theta}_2^-) &= L_C^+(\theta_1^+, \theta_2^+, \dot{\theta}_1^+, \dot{\theta}_2^+), \\ L_H^-(\theta_1^-, \theta_2^-, \dot{\theta}_1^-, \dot{\theta}_2^-) &= L_H^+(\theta_1^+, \theta_2^+, \dot{\theta}_1^+, \dot{\theta}_2^+). \end{aligned} \tag{2}$$

Since $\theta_1^- = \theta_1^+$ and $\theta_2^- = \theta_2^+$, from Eqs. (2) we can get

$$\begin{cases} \dot{\theta}_1^+ = g_1(\theta_1^-, \theta_2^-, \dot{\theta}_1^-, \dot{\theta}_2^-), \\ \dot{\theta}_2^+ = g_2(\theta_1^-, \theta_2^-, \dot{\theta}_1^-, \dot{\theta}_2^-). \end{cases} \tag{3}$$

Thus, the mathematical model of the passive walker has been built, which includes ordinary equations (1) and algebraic equations (3). If a periodic gait exists, a Poincaré map F can be formed by the equations of motion and the transition of state variables. If the Poincaré section is defined at the instant just after each heelstrike, following Garcia,[3] the number of state variables of $\theta_0 = [\theta_{10}, \theta_{20}, \dot{\theta}_{10}, \dot{\theta}_{20}]^T$ can be reduced from four to three, because we have $\theta_{10} = -\theta_{20}$ at that time. Therefore, if the gait is periodical, the group of state variables $[\theta_{10}, \dot{\theta}_{10}, \dot{\theta}_{20}]^T$ is a fixed point of the Poincaré map. Newton–Raphson iteration has been used to find the fixed point, and the stability of the fixed point can be quantified by the eigenvalues of the Jacobian matrix.[1,3,8] Interestingly, a model with a given set of parameters on a slope with a given angle may not have more than one stable gait.[4] However, there is a problem to be solved: the initial state variables of the iteration have to be guessed which often do not converge if the guessed values are not close enough to the fixed point. Thus, we will determine the fixed point of the parameter combinations by the use of the cell mapping method.

3. Cell Mapping Method

The cell mapping method is a global analysis tool, and can be used for determining the basin of attraction of a nonlinear system.[21] Schwab and Wisse[8,14] have applied the cell mapping method to the simplest passive model and obtained a small, pointy boomerang-like basin of attraction. However, investigating the basins of attraction of the general model in Fig. 1 might be more significant for building a prototype. If a model has a large basin of attraction, it will not be sensitive to the initial conditions, and that means it is easy for the prototype to walk. The state variable space is infinite, and we cannot test each point in this space as an initial condition. Thus, we have to discretise this space, using cells to describe the group of points that have the same characteristics.

Before discretising the unlimited state variable space into a finite number of cells, we should ensure the boundary of the space, since the space has physical meaning. It is easy to make certain that leg angle θ_{10} belongs to $[0, \pi/2)$, but the intervals of angular velocities are not easy to estimate. After some trial computations, the feasible state space can be set as follows: $\theta_{10} \in [0, 0.8]$, $\dot{\theta}_{10} \in [-1, 0.2]$ and $\dot{\theta}_{20} \in [-1, 1]$. The feasible initial condition space will be subdivided into a large number (N) of small cells called regular cells, and the condition outside the feasible state space will be called the sink cell.

The sink cell is numbered as 1 and the regular cells are numbered from 2 to $N + 1$. All regular cells are classified into three kinds of cells: virgin cells, cells under processing and processed cells. All the regular cells are virgin cells before a sequence of mapping. Processed cells that have the same periodical characteristics will be assigned the same positive integer group numbers. All virgin cells have 0 as their group number before a sequence of mapping. Cells under processing have a group number of -1 temporarily. Cells will have positive integer group numbers after they have been processed. The group number 1 is assigned to the sink cell.[21]

Now, let us begin the cell mapping from any one of the virgin cells, supposing the number is k. Using the centre of cell k as the initial conditions of the mapping F, the following sequence should be implemented:

$$k \to F(k) \to F(F(k)) \to F(F(F(k))) \to F^4(k) \cdots. \tag{4}$$

After each step, a cell will be mapped to another cell, and the group number of the resultant cell should be checked. If the group number of the resultant cell is 0, it is changed to -1 and the mapping is continued. Otherwise, the sequence is terminated. If a group number of a positive integer is encountered, the group number of all the cells in this sequence should be assigned to this positive integer. If a group number of -1 is encountered, a new periodical motion is found and all the cells in this sequence should be assigned to a new group number of the positive integer. This sequence is

https://doi.org/10.1017/S0263574708004906 Published online by Cambridge University Press

Table II. Some results of cell mapping.

k	$F(k)$	θ_{10}	$\dot{\theta}_{10}$	$\dot{\theta}_{20}$
1041	8977	0.02	−0.24	0.5
3196	6378	0.08	−0.14	0.38
6378	*6378*	*0.18*	*−0.28*	*−0.26*
7055	*7055*	*0.2*	*−0.28*	*−0.22*
7705	7055	0.22	−0.30	−0.22
8977	7705	0.26	−0.36	−0.30

continued until all the cells are processed. All the periodical motion of the system can be found by the aid of the cell mapping method, not only period-one, but also period-k. The accuracy of the cell mapping method depends on the discretisation of the state space.[21] The cells that can be mapped to themselves are called periodical cells. Setting the state variables of periodical cells as the initial value of iteration, a fixed point can be obtained. An example is given in Table II. Setting the values of periodical cells numbered 6378 and 7055 as the iteration initial values, two fixed points can be obtained. One is $\theta_{fp1} = [0.169, -0.262, -0.248]$, an unstable fixed point that has a maximum eigenvalue of 2.0977, and the other is $\theta_{fp2} = [0.202, -0.284, -0.226]$, a stable fixed point that has a maximum eigenvalue of 0.65439.

By the use of the cell mapping method, we have computed the periodical cells of the parameter combinations of Table I. Based on these periodical cells, fixed points were obtained, and the leg angles of the results of $k_r = 0.2$ are listed in Table III. The results of other k_r values are omitted.

The basin of attraction is composed of all the cells that can be mapped to the periodical cells. If the size of the cell is small enough, the basin of attraction is sufficiently accurate. Beginning from any point of the basin of attraction, the motion can converge to the periodical cycles. Unlike the simplest model, which has two state variables, our model has three state variables when the Poincaré section is defined at the instant just after each heelstrike. The discretisation of the 3D state space will result in a large number of cells and the computation time will be too long. Therefore, FORTRAN language was chosen instead of Matlab to increase the computation speed. In addition, the feasible initial condition space was tuned carefully to economise CPU time. The accuracy of the cell mapping method is relevant to the size of cells, but a small cell size conflicts with the computation time. Thus, many trial computations were executed, and a moderate cell size has been chosen. The comparison of different cell numbers is shown in Fig. 2. The upper and the lower panels were obtained from 251,992 cells and 1,234,322 cells, respectively. We can see that there is no significant difference between the high cell numbers and relatively low cell numbers. Therefore, we chose a relatively low number of cells to speed up our computation, and the speed was about 150,000 cells per hour on a P4 2.40 GHz computer.

4. Effect of Parameter Variation on the Gait: Simulation

4.1. On some gait descriptors

From Fig. 3, we can see that the step length $L_{\text{step}} = 2C_2C_1' = 2(C_2C_1 + C_1C_1')$. Since we have $|\theta_1| = |\theta_2|$ on the Poincaré section, the step length can be expressed as $2(2(l-r)|\sin(\theta_1)| + 2r|\theta_1|)$. In the interval of the leg angle we discussed, the step length is the monotonic increasing function of the leg angle θ_1, which is the first element of the fixed point. We use the leg angle to represent the step length, and the trends of leg angles along the foot radius are shown in Fig. 4. The vertical axis is the leg angle, and the horizontal axis is the non-dimensional moment of inertia k_J. For a given set of values of k_c and k_r, the leg angle of the fixed point grows with the increasing k_J. This means the step length of the model increases with the increasing moment of inertia. However, period-doubling will occur when k_J grows large enough. Moreover, if k_c and k_J are fixed, the step length grows with the increasing foot radius k_r. Furthermore, a larger k_c may result in a small step length when k_J and k_r are fixed.

Since our dynamic equation is dimensionless, the period is also non-dimensional. For small values of k_J, the periods of the gaits decrease with the increasing k_c when k_c is small, but later grow with the increasing k_c, while the other parameters are kept constant, as shown in Fig. 5. However, along with the increase of k_J, the inflexion of the decreasing–increasing trend of the period is postponed gradually, and eventually reaches a steady decreasing trend. This increase of k_J will result in a significant increase of the period, but the effect of k_r is not very clear. Thus, we show the period in the sequence of k_r, as shown in Fig. 6. In most cases, the period grows with the increasing k_r, while k_c and k_J remain constant. However, in some cases, the increase of k_r does not have a significant effect on the increase of the period, and some exceptions also exist, especially when k_J is small. The trend of the period along k_r is not in accordance with the results of Asano and Luo.[15] From personal communications, we have agreed that the difference is caused by the difference of models. Our model is a pure passive model, and Asano's model is an actuated one.

Table III. Leg angles of fixed points of $k_r = 0.2$.

$k_c \backslash k_J$	0.01	0.02	0.04	0.06	0.09	0.12	0.16
0.1	0.207	0.239	0.274	0.294	Pd[a] at $k_J = 0.082$	–	–
0.2	0.190	0.209	0.238	0.25	0.272	0.285	Pd at $k_J = 0.13$
0.3	0.182	0.194	0.213	0.228	0.245	0.257	Pd at $k_J = 0.15$
0.4	0.169	0.178	0.194	0.206	0.221	0.233	Pd at $k_J = 0.14$
0.5	0.151	0.159	0.173	0.184	0.198	Pd at $k_J = 0.11$	–
0.6	0.128	0.136	0.149	0.160	Pd at $k_J = 0.08$	–	–
0.7	0.101	0.110	Pd at $k_J = 0.034$	–	–	–	–

[a]Pd indicates the occurrence of period-doubling.

https://doi.org/10.1017/S0263574708004906 Published online by Cambridge University Press

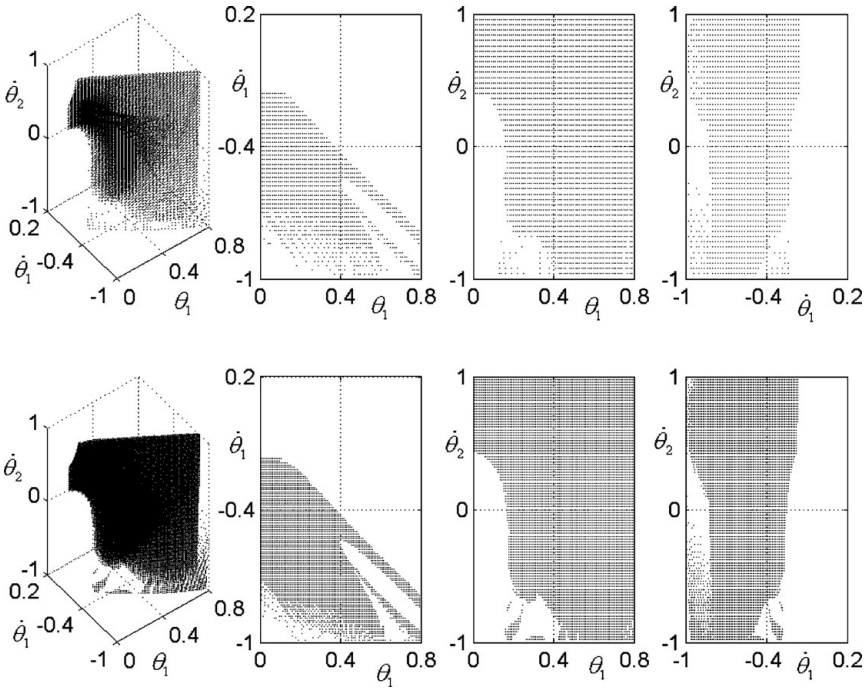

Fig. 2. Basin of attraction of different cell numbers.

The hip speed of the model along the slope varies every time during walking, thus we let the models walk at the same time, and recorded the displacement they moved along the slope, and used the average speed to represent the velocities. As shown in Fig. 7, it is clear that the speed increases with the increasing k_r. When k_c and k_J are small, it seems to result in a high average speed, but this is not very clear. We show the average speed in the sequence of k_c, as shown in Fig. 8. We can see that the average speed decreases with the increasing k_J, and increase with the growing k_c, but exceptions occurred when the k_c was small.

For a passive walking model, energy loss only occurs at the heelstrike. The common dimensionless measurement of inefficiency[21] for walking is

$$\eta = \frac{\text{Energy dissipated per step}}{\text{(Walker weight)} \times \text{(Step length)}}.$$

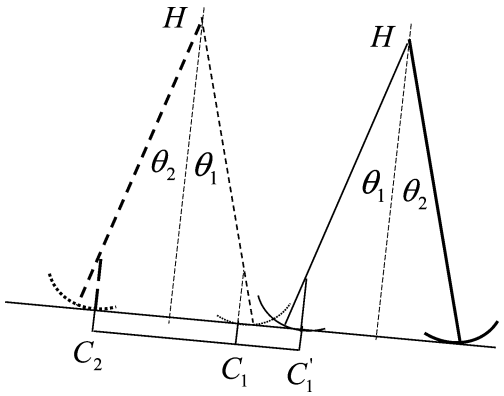

Fig. 3. Half step length of the model.

Table IV. Effect of parameters on the gait.

	Step length	Period	Speed	Inefficiency
When k_c ↗	↘	↗*	↘[a]	–
When k_J ↗	↗	↗	↘	–
When k_r ↗	↗	↗*	↗	–

[a]Indicates there are some exceptions.

Since the model is powered only by gravity, the energy dissipated per step is (weight) × (height drop over one step). Thus the inefficiency measure can be reduced to $\eta = \sin\gamma$ if the step length is along the slope.[3] Therefore, the inefficiency measure η is independent of the parameters of k_c, k_J and k_r. Our simulation results also indicate this.

We summarise the effect of parameters on the step length, period, speed and inefficiency in Table IV.

4.2. On basins of attraction

A model with a stable gait that has a large basin of attraction means that this gait can start from points far from the fixed point. In other words, this model is not sensitive to the initial conditions. Thus, models that have large basins of attraction might be significant not only in simulations but also in experimental settings. However, as mentioned earlier, using the cell mapping method to obtain the basin of attraction is time-consuming work. Thus, we did not process all the combinations of the parameters as shown in Table I, but chose some other ones. Since the state space is a 3D space, we also drew the projections of the basins of attractions on three-coordinate planes.

First, we investigate the effect on the basin of attraction of the change of foot radius. We can see that the basin of attraction grows larger with the increasing foot radius, when $k_c = 0.25$ and $k_J = 0.02$. Further computations also indicate that the increasing foot radius has a positive effect on the

https://doi.org/10.1017/S0263574708004906 Published online by Cambridge University Press

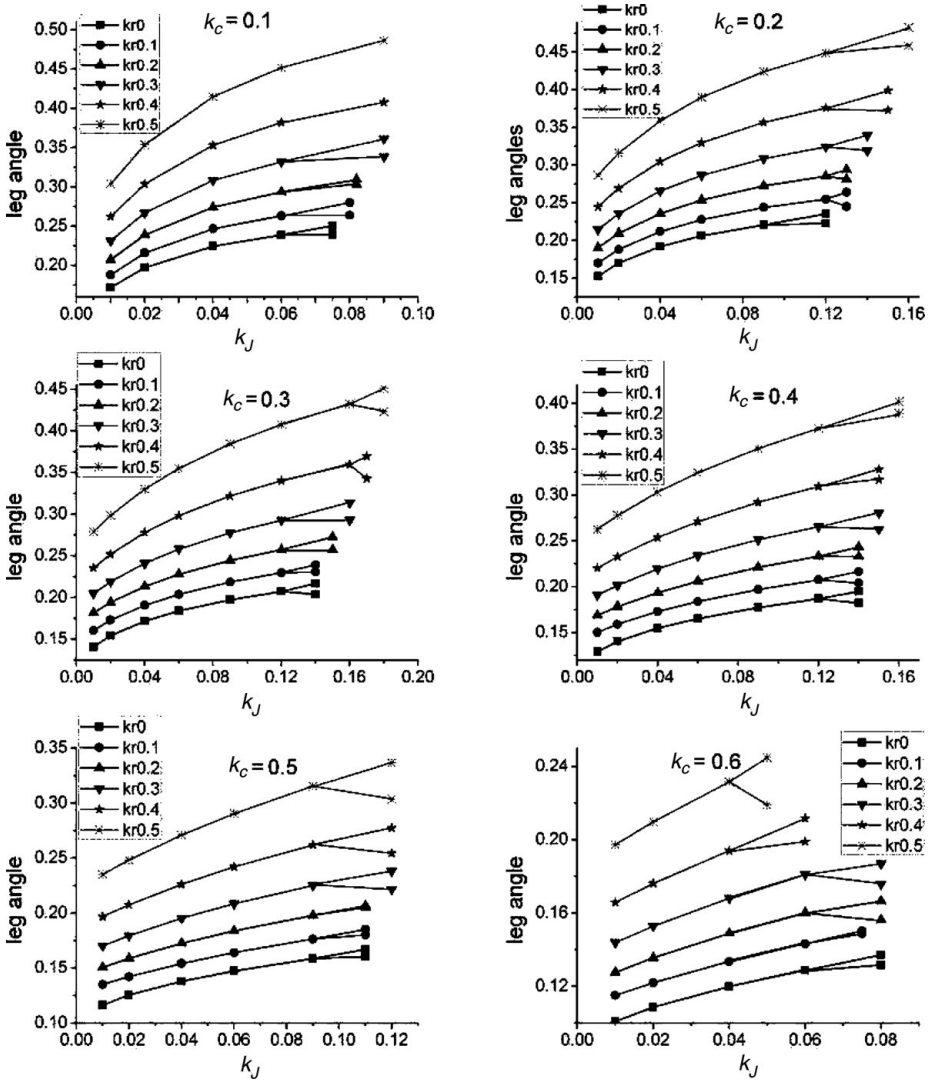

Fig. 4. Leg angles at the fixed point of different parameters.

area of the basin of attraction when other parameters are kept constant. In Fig. 9, the feasible region has reached the boundary of the state variable space, and we will discuss a larger state space later.

The increase of the moment of inertia seems to have a negative effect on the area of the basin of attraction, as shown in Fig. 10. However, in our results, the largest area of basin of attraction does not appear at the minimum value of k_J, but at the value of 0.02 or 0.04. When k_J approaches zero, the basin of attraction vanishes quickly. When k_J grows much larger, the basin of attraction gradually becomes sparse and small. The basins of attraction of other parameter combinations also indicate the same phenomenon.

The effect on the basin of attraction of the changing of the centre of mass is a bit complex. For the point foot model, the increase of k_c may cause a decrease of the basin of attraction. However, for models with round feet, the basin of attraction grows with the increasing k_c, as shown in Fig. 11. Similar phenomena also appear during computations of models that have different k_J or k_r.

From the results discussed earlier, we summarise the rules of tuning the parameters to enhance the basin of attraction: (1) enlarging the radius of the round foot, (2) choosing a relatively small dimensionless parameter of the moment of inertia k_J, which is about 0.02 and (3) finding a moderate dimensionless parameter of the centre of mass k_c, for which 0.2 or 0.3 might be better.

According to these rules, we think that the model with the parameters $k_r = 0.5$, $k_J = 0.02$ and $k_c = 0.25$ will work well. Then, we investigate the basins of attractions of this model on different slopes. From Fig. 12, we can see that this model indeed has a relatively large basin of attraction on different slopes. As the slope increases, the basin of attraction decreases slowly.

Furthermore, we will see the basin of attraction of this model without the limit of angular velocities. Based on common sense, we set $l = 1\,\mathrm{m}$, and then the results will be dimensional, as shown in Fig. 13. The stable fixed point $\theta_{\mathrm{fp}} = [0.2377, -1.2719, -0.9478]$ is marked by "*," and some special points are marked by "▲." These special points will now be discussed.

First, the periodical gait of the model can begin from a point far away from the fixed point. As mentioned above, McGeer's model can absorb a perturbation of 150% of one initial angular velocity, and at the same time, the other angular velocity can only tolerate a few percent errors.[1] Goswami

https://doi.org/10.1017/S0263574708004906 Published online by Cambridge University Press

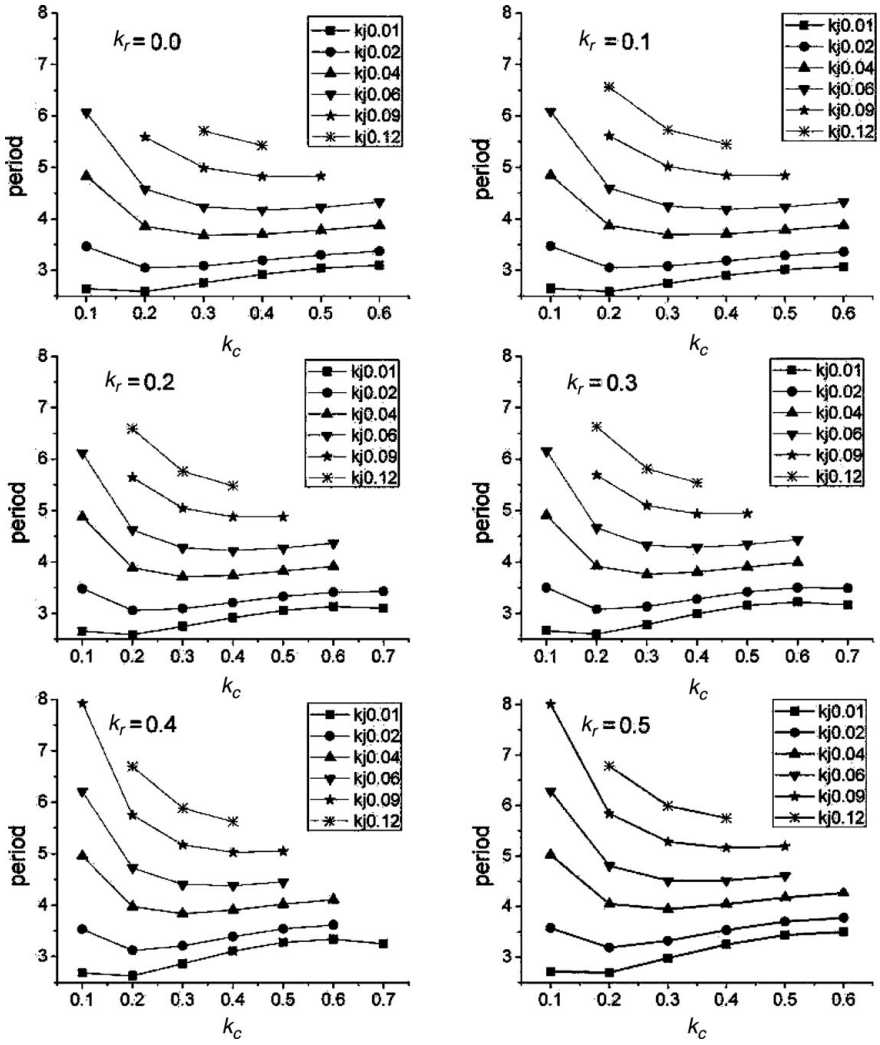

Fig. 5. Gait periods of different parameters in the sequence of k_c.

et al.[4] have reported an example in which the angular velocity can be more than 100 deg/s, whereas the change of angle must be limited to 2°. For our model, the coordinates of point 1 is [1.2000, −3.0695, −3.2574]. Compared with the fixed point [0.2377, −1.2719, −0.9478], the angle was more than 400%, about 55°. Both the angular velocities were more than 100 deg/s. From Fig. 14 (upper panel) we can see the development of the state variable from point 1. Second, the repetitive steps can start from the state in which both legs are perpendicular with the slope, represented by point 2 in Fig. 13. Although the model will be statically unstable at this position, it can realise a dynamical stable gait from certain initial conditions, as shown in Fig. 14 (middle panel). Third, when the stance leg falls backward just after heelstrike ($\dot{\theta}_1$ is positive), represented by point 3 in Fig. 13, sometimes the model can still walk if the swing leg moves forward fast, as shown in Fig. 14 (lower panel). Although the problem of avoiding falling backward is still unsolved, because the feasible region is very small, this phenomenon might be worth studying further.

4.3. On robustness

Although a model with a large basin of attraction may not be sensitive to the initial conditions, the robustness of the model is not clearly understood. Robustness is the characteristic of a model during the whole act of walking. Hence, we used random disturbance to discover the robustness of the models. We used two types of random floors to introduce disturbances; one was a random slope angle, and the other was random stairs.

As shown in Fig. 15 (upper panel), the slope angle is γ_0 at the initial position, and it changes to $\gamma_i = (\gamma_0 + \delta_i)$ after the ith step. The perturbation δ_i is obtained from $\delta_i = \frac{|\alpha|}{\alpha} \cdot \varepsilon \cdot \beta[ra, rb]$, where α is a non-zero random number, β is a random number from the interval $[ra, rb]$ and ε is a scaling coefficient (in radians). The initial value of the slope angle is 0.02 rad. The constant ε is set as 0.001, and the interval of random number β is first set as [0, 0.5]. Therefore, δ_i will be a random value of the interval of [−0.0005, 0.0005] rad. It is a very small disturbance. The floor of random height stairs is shown in Fig. 15 (lower panel), the slope also has an initial angle of 0.02 rad, and the height of steps varies stochastically. These stairs are a general form of the stairs used by Ali Tehrani Safa.[22] The interval of h_i is set as [−0.015, 0.015], which is smaller than 1.5% of the leg length, but the maximum height difference might reach 3% of the leg length.

The random disturbance will affect the gait. From Fig. 16 we can see that, on a flat slope, the model will walk stably

https://doi.org/10.1017/S0263574708004906 Published online by Cambridge University Press

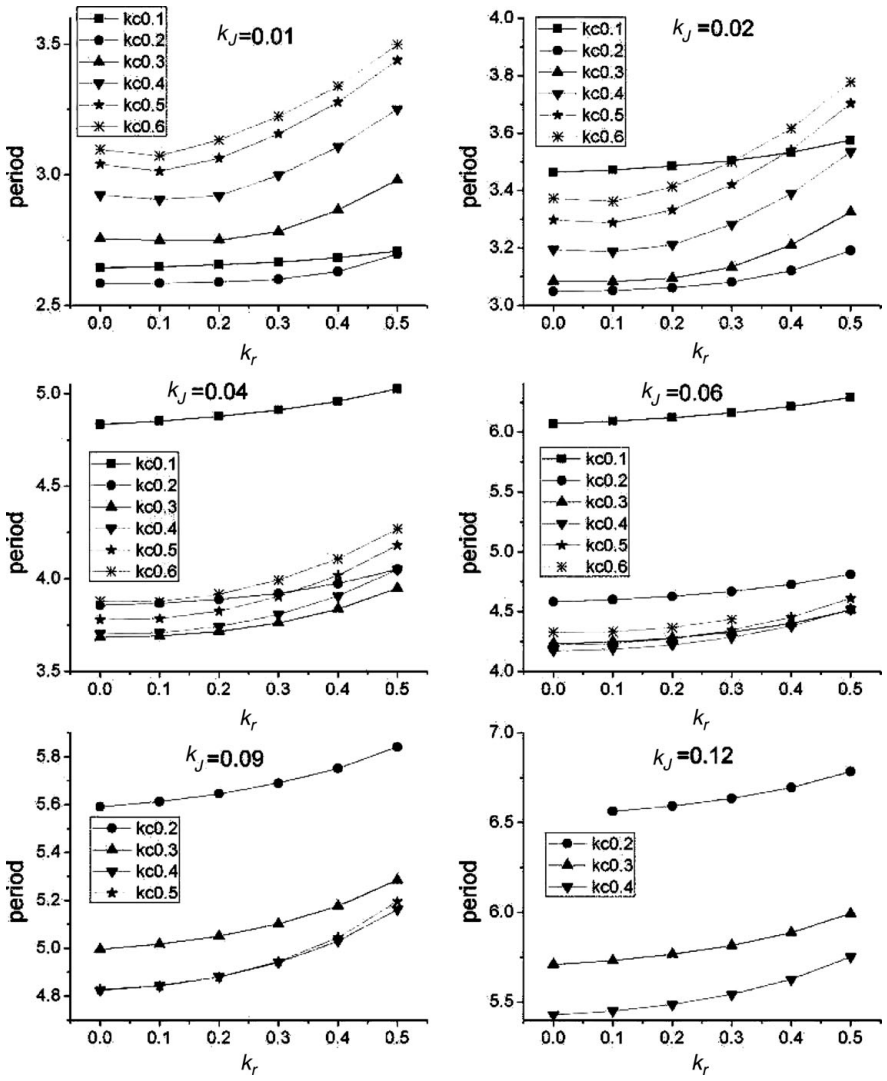

Fig. 6. Gait periods of different parameters in the sequence of foot radius k_r.

(a), or converge to the stable gait if it starts from a fixed point nearby (b). If a random slope angle is introduced, the model can still walk, but each step will not be equal (c), and it can fall (d).

For a model of given parameters, we let it walk many times on the uneven floor, and recorded the number of falls to obtain the fall ratio. Our study was limited to models with stable fixed points. For each model, we generated 500 simulations of 100 non-dimensional time units, and all the simulations started from the fixed point. The intervals of random slope angle and step height were as mentioned earlier.

The fall ratios of the models of different parameters on the floor with random slope angles are shown in Fig. 17, the vertical axis is the percentage, and the horizontal axis is the non-dimensional centre of mass k_c and the non-dimensional moment of inertia k_J. It is very clear that the models with $k_r = 0$ all have fall ratios of 100%; thus, they are not discussed here. For the other charts, we can see that the increasing k_r has a positive effect on the robustness. In each chart, the fall ratio decreases along the axis of k_J; namely, a large k_J may result in a low fall ratio. The changing of fall ratio along the axis of k_c is not monotonous, but a small k_c is good for robustness. A model with a large k_r and k_J, along with a small k_c, will have a very low fall ratio, even as low as zero. The effect of k_J seems more significant. All the models with the value of k_J higher than 0.09, no matter what the values of k_r and k_c are, have fall ratios smaller than 20%. On the other hand, the models with k_J equal to 0.01 have extremely high fall ratios, even if the k_c is small and the k_r is large.

The fall ratios of the models on the floor with random stairs are shown in Fig. 18, in which the vertical axis is the percentage, and the horizontal axis is the non-dimensional centre of mass k_c and non-dimensional moment of inertia k_J. Models with pointed feet fell in all the simulations. Similar to the test of random slope angles, enlarging the foot radius and decreasing the k_c has a positive effect on the robustness. However, a small moment of inertia is needed to decrease the fall ratio, and this phenomenon is opposite to the test of random slope angles.

Therefore, we summarise the parameters of the model that have a low fall ratio in our test: (1) It should have a small value of k_c; (2) a large foot radius might be good for enhancing robustness; (3) the model with a large value of moment of inertia worked well in the test of random slope angle, but in contrast, the model with a small value of moment of inertia had a low fall ratio in the test of random stairs.

https://doi.org/10.1017/S0263574708004906 Published online by Cambridge University Press

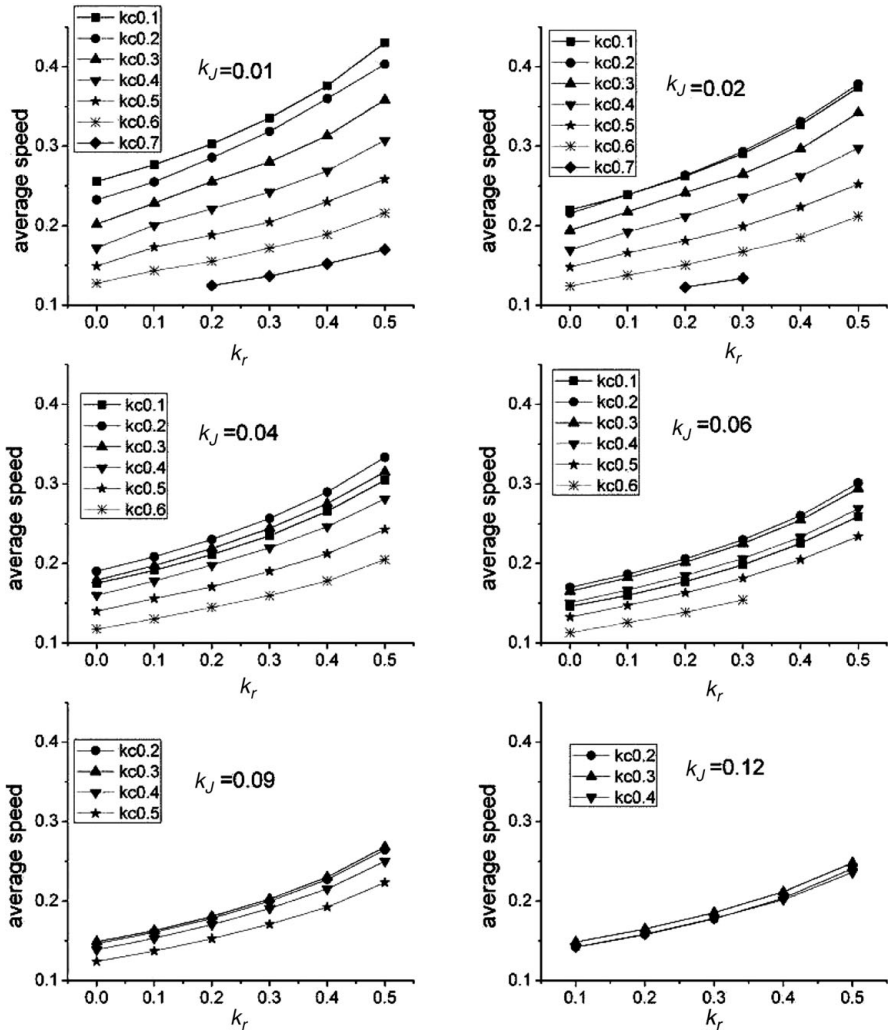

Fig. 7. Average hip speed of models of different parameters along the slope in the sequence of k_r.

5. Experiment

To validate the simulation results, we carried out walking experiments using a prototype. The aluminium-made prototype is shown in Fig. 19. Four types of plastic feet were made, and the centre of mass and moment of inertia could be adjusted by adding or removing bolts on different positions of the legs. To avoid foot scuffing, wood blocks were set on a board 2 m long, and the prototype walked on the blocks. Four bars 2 m in length were fixed on the board to secure the blocks. To fit different step lengths, the distance along the bars of the blocks could be adjusted manually. The friction between the bars and the blocks made the blocks immovable when the model was walking on them. The angle between the board and the horizontal plane was 0.03 rad, a little different from our simulation.

In order to test the model's behaviour with different feet radii, we adjusted the position and number of bolts to make the models have the same k_c and k_J, as shown in Table V. The maximum parameter error between different models was less than 0.5%. The feet were numbered from 1 to 4, from big to small, and could be easily installed on the model. We also used these numbers to distinguish models when different feet were installed.

5.1. Effect of feet radius on the basin of attraction

We want to ensure the prototype can walk; thus the basin of attraction is discussed first. According to our simulation about the basin of attraction, a model with small values of k_c, k_J and a large value of k_r will not be sensitive to the initial conditions; it can easily walk by manual release. This prototype has feet from moderate to large size, but the k_J is large and the k_c is not very small. We have tried to compute the basin of attraction of the model with the parameters given earlier by the cell mapping method; however, no good results were obtained.

Surprisingly, during the experiment, it was not difficult for this model to walk. After some exercises, an experienced person (one of the authors) could operate it easily. We hypothesised that if the same person releases the model manually many times, the model that is not sensitive to the initial conditions will have a high probability of walking a long distance. For each type of model, 100 manual releases were implemented continuously, and the number of steps the models could walk were recorded. Since models with a larger foot radius have a larger step length, Models 1 and 2 could only walk 9 steps on the 2 m-long board, but Models 3 and 4 could walk 10 and 11 steps until they reached the end.

https://doi.org/10.1017/S0263574708004906 Published online by Cambridge University Press

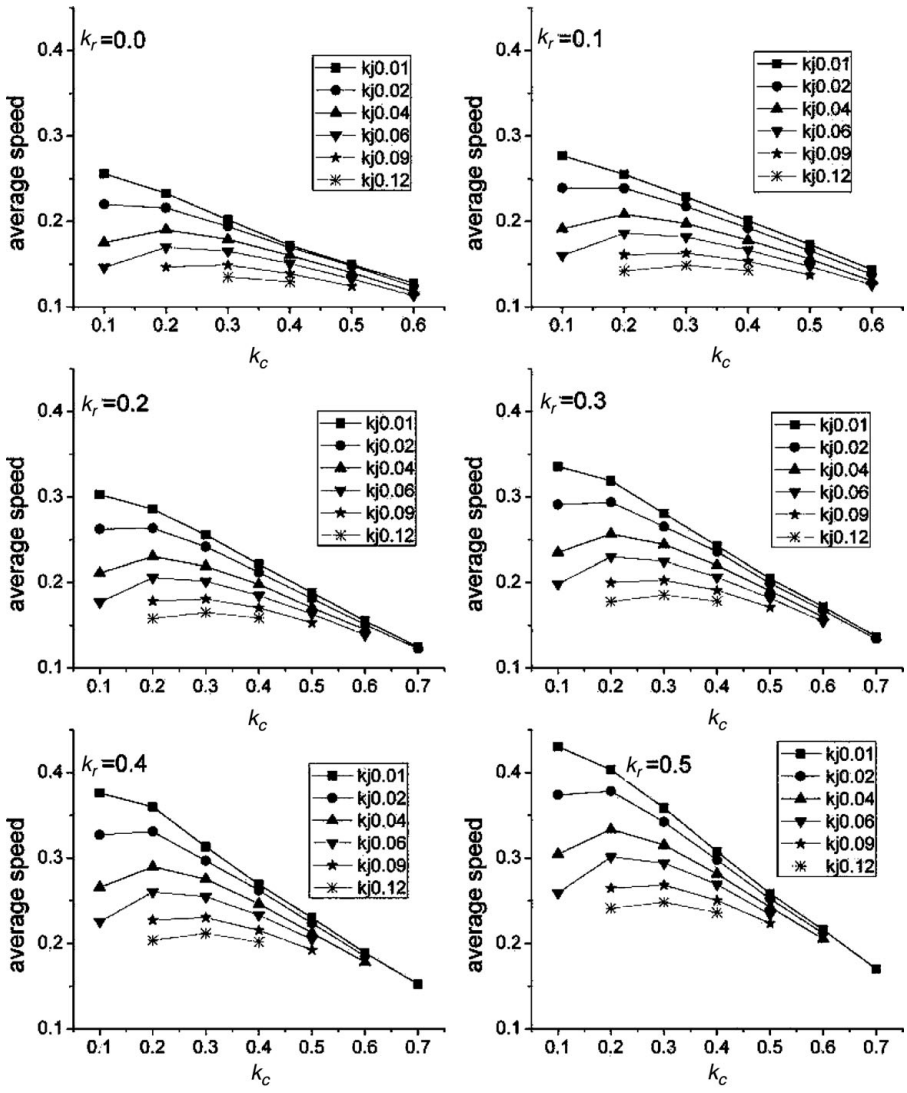

Fig. 8. Average hip speed along the slope in the sequence of k_c.

From Fig. 20, we can see that models with all four types of feet had high percentages of walking to the end of the board. Interestingly, the model with the largest radius feet did not have the highest percentage of reaching the end of the board. For Model 1, only 48% of the 100 trials could walk 9 steps. In contrast, Model 4 reached the end 69 times, and Model 3 reached the end 73% of the time. It seems that this result is not coincident with our simulation, in which the model with a large foot radius has a large basin of attraction. However, if we view it from another angle, Model 1 has a low percentage of falling in the first five steps, but Model 4 has the highest percentage of falling in the first five steps, as shown in Table VI.

If a gait did not start from the fixed point but could converge to the limit cycle, it often converged in the first several steps. This phenomenon was proven by many walking simulations, and can be found in Figs. 14 and 16(b). Thus, during experiments, if the model walked five steps, we hypothesised that it had converged to a stable gait. From Table VI, we can see that, for Model 4, many falls occurred in the first five steps. Therefore, a large foot radius is good for the model to converge to a stable gait. However, we should try to explain

Table V. Parameters of the models with different foot radii.

Feet	1		2		3		4	
Leg length (m)	0.324							
Leg type	Outer	Inner	Outer	Inner	Outer	Inner	Outer	Inner
Foot radius (m)	0.15		0.12		0.09		0.06	
k_r	0.4630		0.3704		0.2778		0.1852	
k_c	0.4264	0.4269	0.4269	0.4265	0.4270	0.4267	0.4267	0.4268
k_J	0.1184	0.1188	0.1184	0.1185	0.1185	0.1183	0.1182	0.1182
Mean k_c	0.42673							
Mean k_J	0.11841							

https://doi.org/10.1017/S0263574708004906 Published online by Cambridge University Press

Table VI. Step recording for walking experiments.

Foot & steps	1	2	3	4	5	6	7	8	9	10	11	Sum	Times of falling in the first five steps
1	0	3	4	4	2	8	12	19	48	–	–	100	13
2	2	1	3	7	3	11	4	9	60	–	–	100	16
3	0	2	8	2	5	2	2	6	0	73	–	100	17
4	3	0	16	3	2	2	4	1	0	0	69	100	26

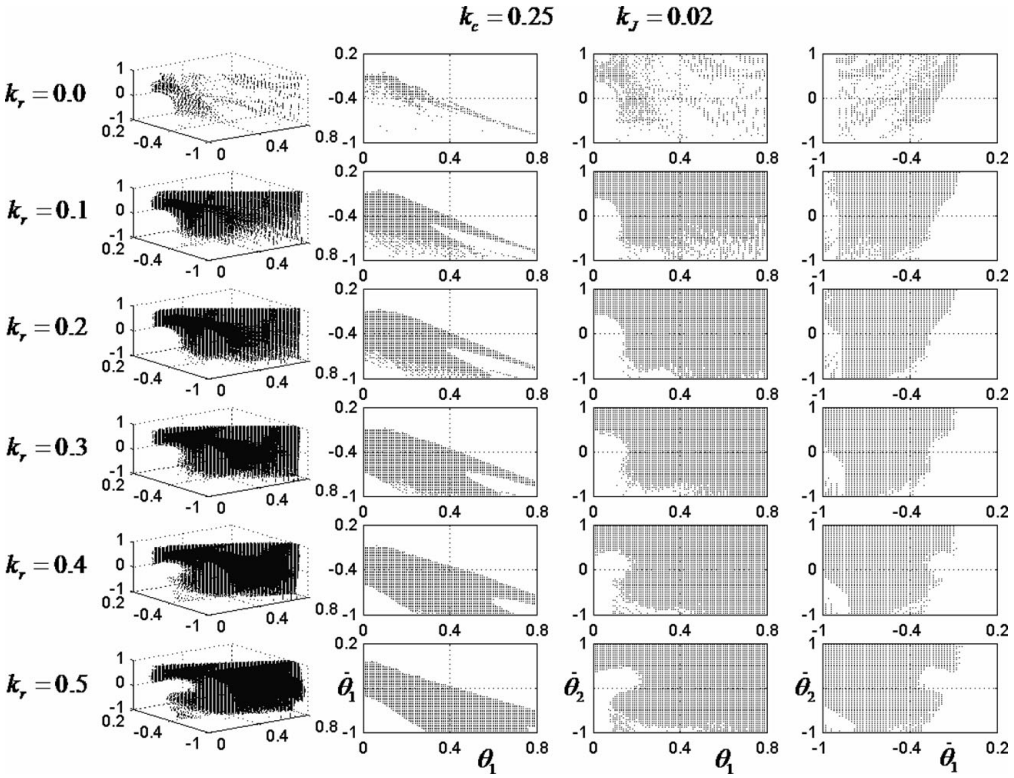

Fig. 9. Basins of attraction and their projections with the increase of foot radius.

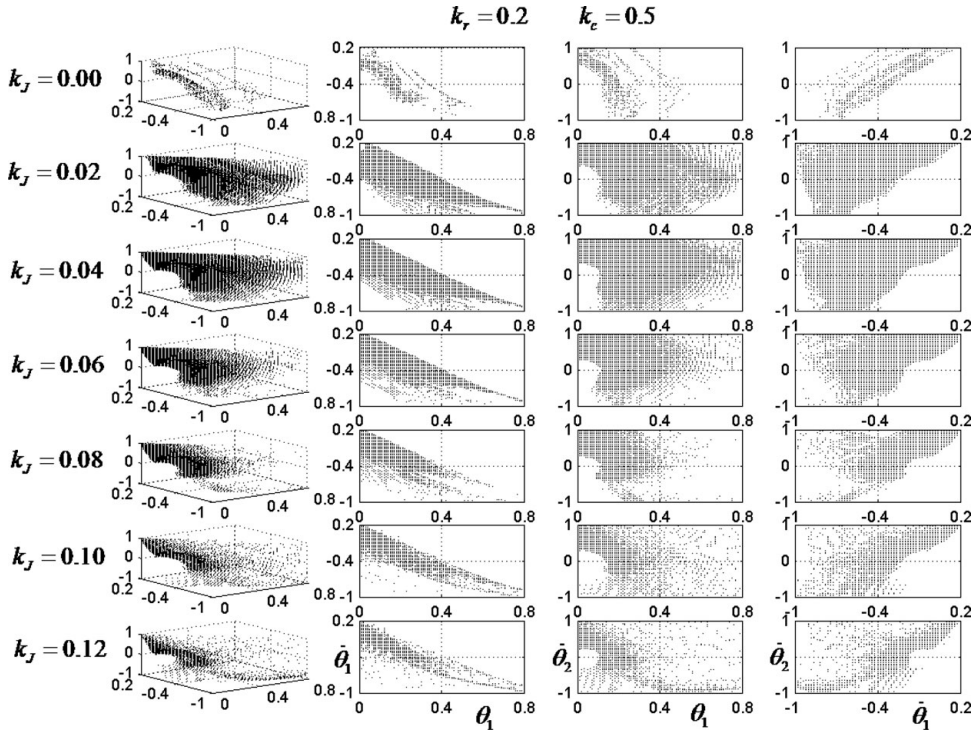

Fig. 10. Basins of attraction and their projections with the increase of moment of inertia.

https://doi.org/10.1017/S0263574708004906 Published online by Cambridge University Press

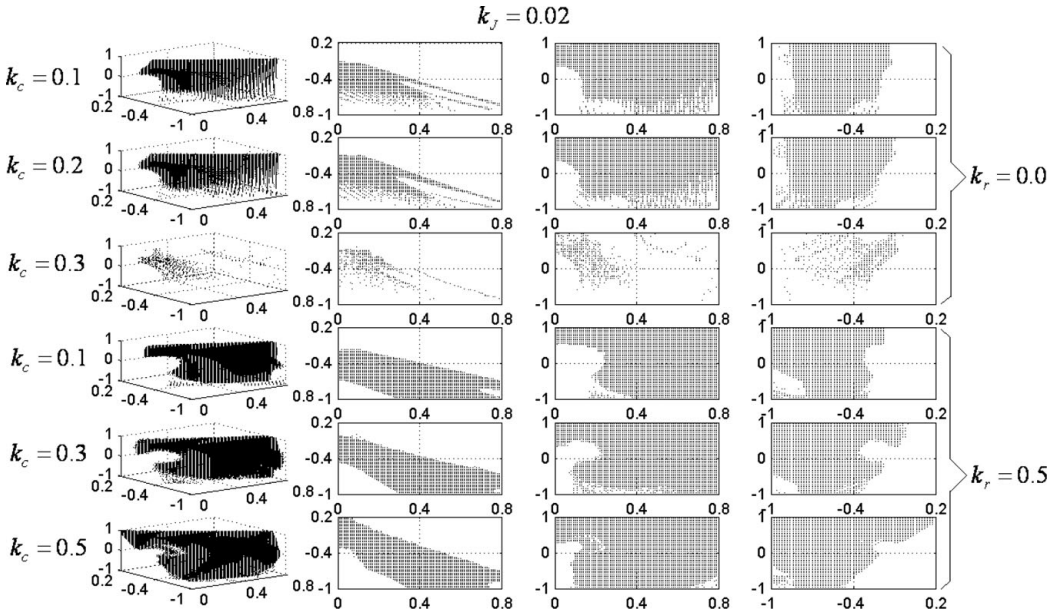

Fig. 11. Basins of attraction and their projections with the increase of centre of mass.

why Model 1 fell many times just one or two steps before the end.

When walking stably, the model with larger feet has a larger leg angle at heelstrike, and the ground reaction force acting on the feet has a larger arm relative to the joint between the foot and the leg. This torque caused by the reactive force may result in the feet rotating around the ankle, and the model will not be symmetric, as shown in Fig. 21. During the experiment, this design flaw appeared in every trial of Model 1, and became serious in the final few steps. We had to adjust the model manually after each trial. However, for models with smaller feet, this problem was not very serious, and the models only had to be adjusted after many times of trials. We think this is the main reason that Model 1 fell many times just before the end.

5.2. *Effect of foot radius on other gait descriptors*

As listed in Table IV, the simulation results indicate that the increase of foot radius has a positive effect on the step length, gait period and average speed. We selected the trials in which the models had reached the end of the board to record the gait data. From Table VII, we can see that the step

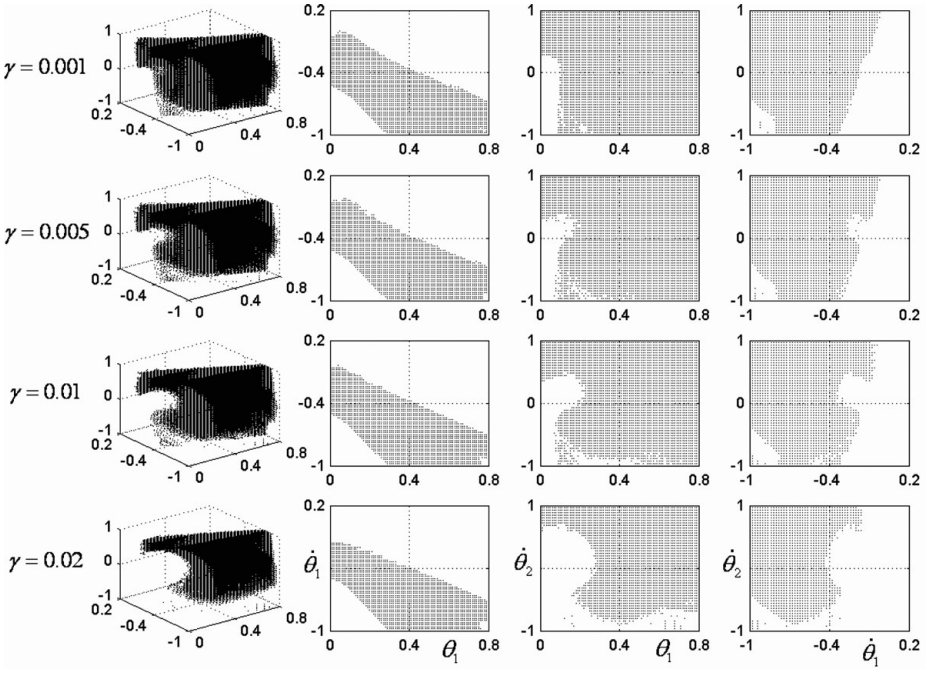

Fig. 12. Basins of attraction and their projections with different slope angles.

https://doi.org/10.1017/S0263574708004906 Published online by Cambridge University Press

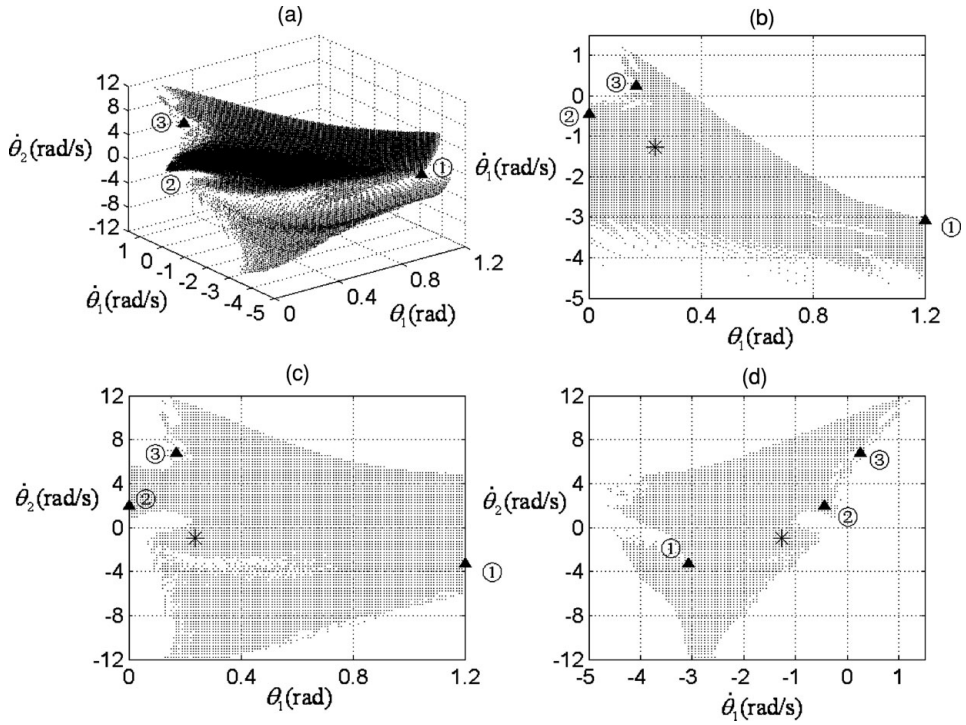

Fig.13. Basin of attraction and its projections for the model without angular velocity limit.

lengths of experiment are not very consistent with those of the simulation, especially for Model 1. We think the foot–leg configuration change caused by the ground reaction force is the reason for the difference between the experimental and the simulation results. For Models 2–4, the effect of enlarging the foot radius to increase the step length was validated by experiments. The experimental results were smaller than the simulation results. We used the board length divided by the step numbers to obtain the mean step length; however, in the trials, walking did not start exactly at one end of the board and end at the other endpoint exactly; thus, the full walking distance was shorter than 2 m.

We recorded the sounds of the steps to obtain the time of walking to the end. The sound recording started from the first time of heelstrike; thus, the time of the first step was not included, and the mean time of walking to the end did not represent the whole time of walking. If we neglect the time differences of the first step among the four, the mean

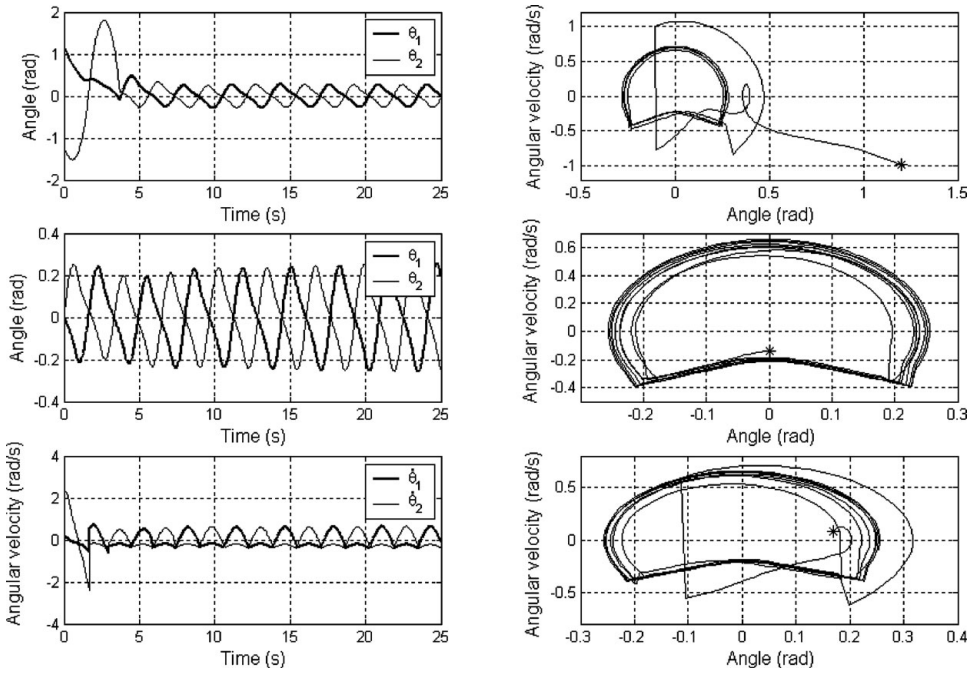

Fig. 14. State variables and phase portraits of the model beginning from certain initial conditions.

https://doi.org/10.1017/S0263574708004906 Published online by Cambridge University Press

Table VII. Simulation and experimental results for the gaits of the prototype with different feet.

Model		1	2	3	4
Simulations	Fixed point				
	θ_1(rad)	0.3973	0.3351	0.2909	0.2573
	$\dot{\theta}_1$(rad/s)	−2.6533	−2.3963	−2.1977	−2.0359
	$\dot{\theta}_2$(rad/s)	−1.8758	−1.7548	−1.6447	−1.5468
	Period (s)	0.5186	0.5082	0.5016	0.4974
	Step length (m)	0.2538	0.2146	0.1866	0.1652
	Average speed of 10 steps (m/s)	0.4704	0.4065	0.3550	0.3174
Experiments	Number of steps when reaching the end	9	9	10	11
	Mean step length (m)	0.2222	0.2222	0.2000	0.1818
	Mean time of walking to the end (s)	4.0430	4.2264	4.4852	4.9684

time of walking to the end still indicates that the model with the smallest foot radius walked the slowest. As listed in Table VII, the period data of the simulations are close to each other, and we cannot distinguish them from the experiment data.

5.3. Experiment of robustness

In the simulation, we used floors of random slope angle and random stairs to test the robustness of the models, and set the fall ratio as a measurement. We have found that a large foot radius may be beneficial for walking on uneven floors. During the experiment on flat floors, there were many random disturbances, such as the roughness of the blocks, the asymmetry of the prototype, assembly errors and the foot rotation about the ankle joint caused by ground reaction forces. However, they were not too serious, except for the last one, which affected Model 1. Disturbed by all of these perturbations, the models still reached the end of the flat floor more than 45% of the times, and the highest percentage was 73%.

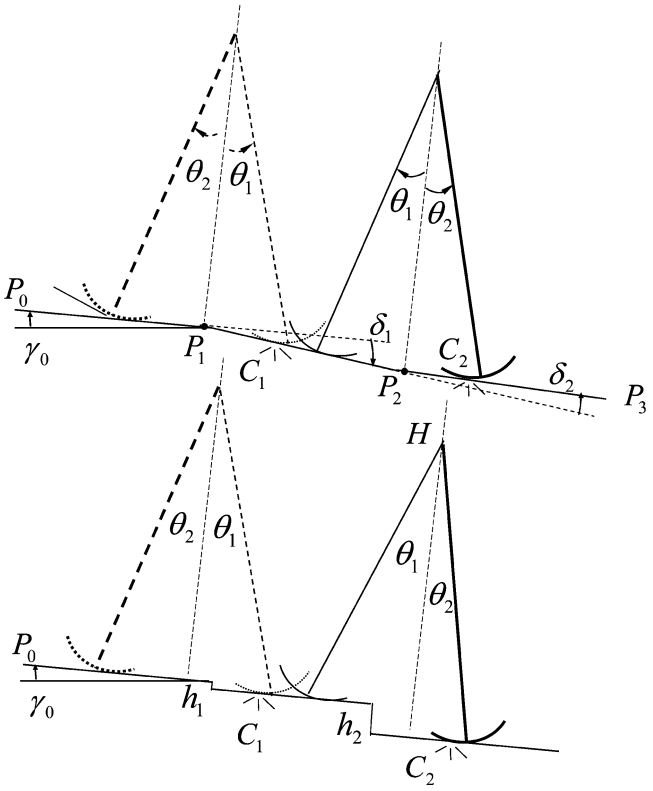

Fig. 15. Sketch maps of uneven floors.

We pushed thumbtacks into the block to construct a random slope angle floor, as shown in Fig. 22. The thickness of the head of each thumbtack was 0.2 cm, which made the block to have a slope angle of about 0.03 rad when the edge touched the floor. However, the blocks were clamped tightly by the bars and could not rotate freely unless some force pushed them. Since we released the models manually, when the model tread on the block, the position of the contact was uncertain; thus the angle of the block could rest at any angle equal to or smaller than 0.03 rad. After each walking trial, we did not reposition the blocks. Therefore, in the next trial, the feet may have tread on positions different from the last time. We used this type of approximate random slope angle floor to test the models.

In the experiment, the models were released manually, and could not walk more than 12 steps, restricted by the length of the board. We assumed that if the model could walk four steps, it had converged to a stable gait; otherwise, the fall might have been caused by a bad release. From the fifth step, thumbtacks were tacked into the blocks, and random disturbance was introduced. For each type of foot radius, many walking trails were implemented, and 100 times of walking trials that were more than four steps were recorded, as shown in Fig. 23. The wedges representing the trials in which the model reached the end of the board are magnified. We can see that the step length was changed, and Models 2 and 3 could walk more steps until they reached the end than when they were walking on a flat floor.

Model 1 does not have the highest pass ratio; however, it has a significantly higher percentage of trials in which it fell one step before the end. We think that the change of configuration caused by the ground reaction force still plays a key role. Model 2 has the highest ratio of reaching the end. However, the ratio of reaching the end for Model 4 is a bit higher than the ratio of Model 3. This phenomenon can be explained as follows. As shown in Fig. 22, the distance of foot 3 rolling on the block is longer than the distance of foot 4, from one side of the thumbtacks to the other side; thus, the block may be forced to rotate. Therefore, the models with larger feet have extra disturbances of block angle changes when their feet are rolling on the blocks. In this test, the effect of increasing the foot radius on enhancing the robustness of the models has been validated.

https://doi.org/10.1017/S0263574708004906 Published online by Cambridge University Press

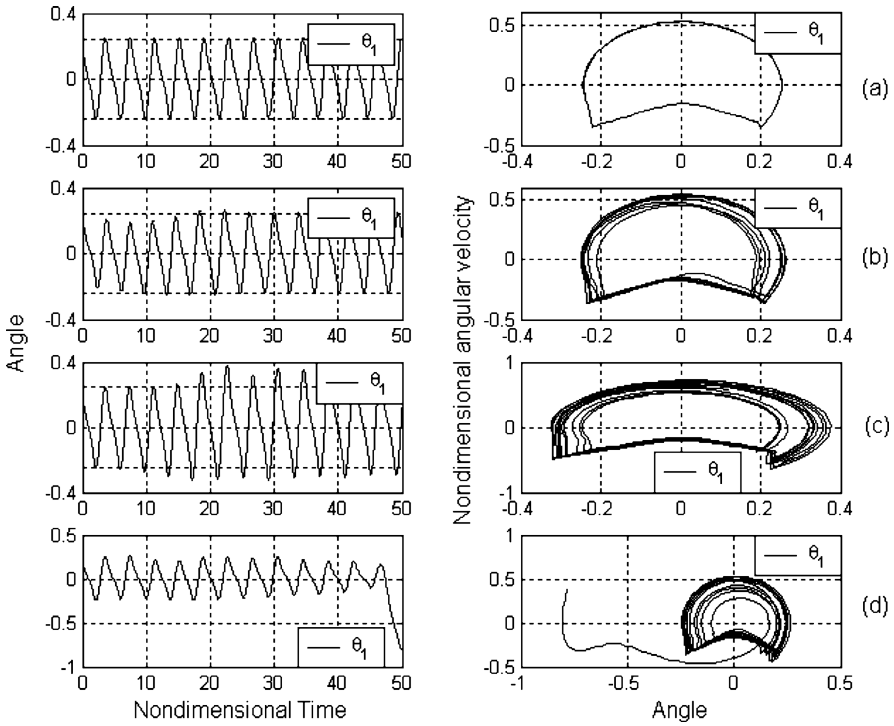

Fig. 16. Leg angles and phase portraits of models with and without slope angle change.

6. Conclusion and Future Work

We have made a systematic study of the effect of parameters on the gait of a planar passive walker with straight legs and

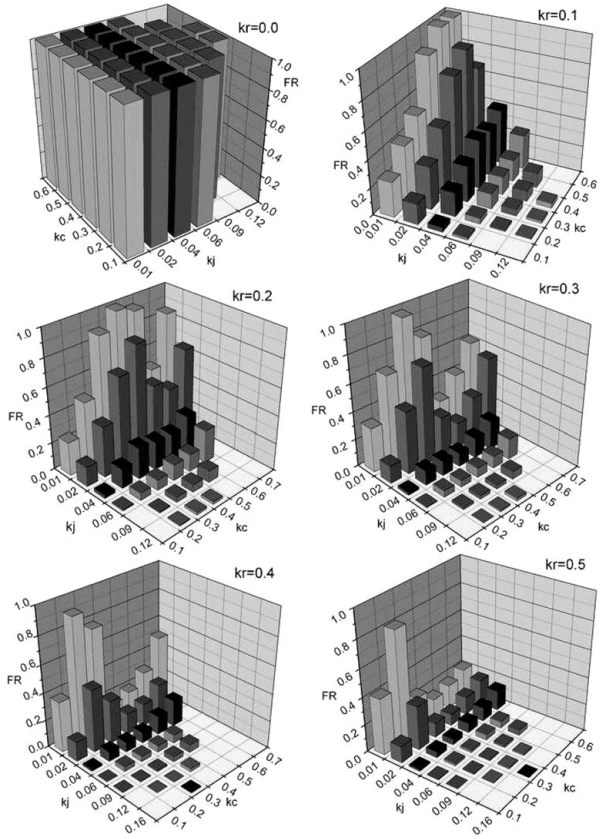

Fig. 17. Fall ratios of models of different parameters on a floor with random slope angles.

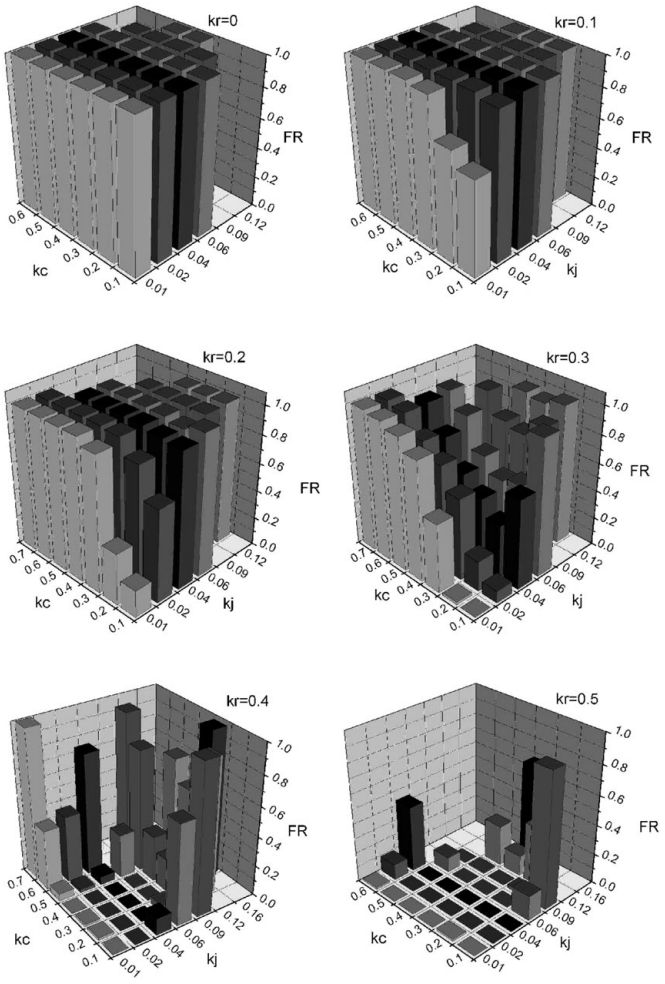

Fig. 18. Fall ratios of models with different parameters on a floor with random stairs.

https://doi.org/10.1017/S0263574708004906 Published online by Cambridge University Press

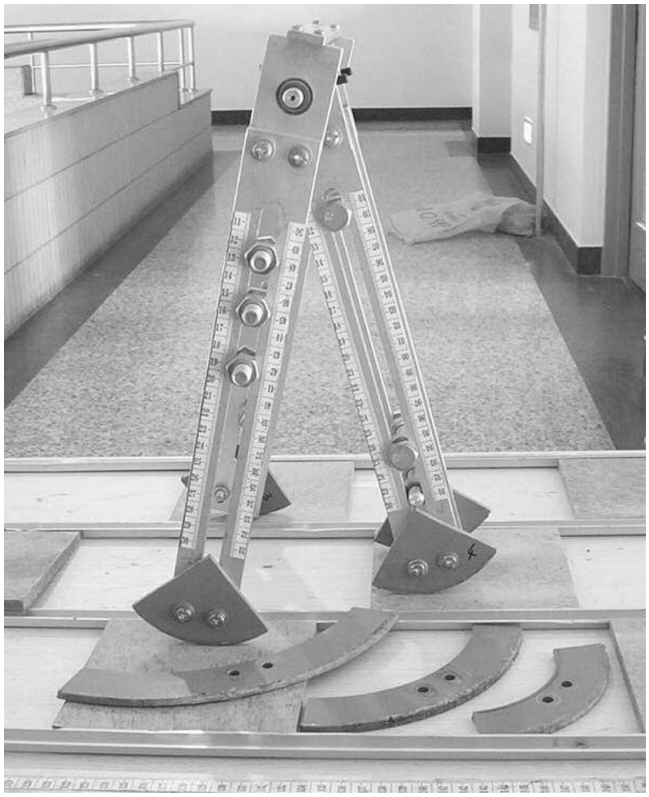

Fig. 19. The prototype and different feet.

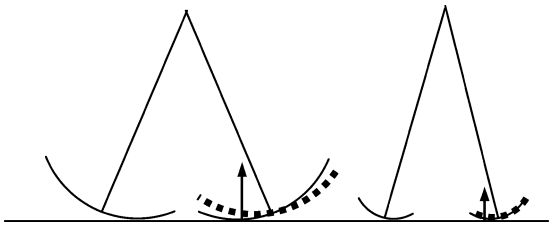

Fig. 21. Ground reaction force may cause the feet to rotate around the joint.

round feet. Our objective was to provide a guide for building a robust prototype that can walk stably. Different from former researchers, we chose three non-dimensional parameters, k_c, k_J and k_r, representing the centre of mass, the moment of inertia and the foot radius, respectively. We treated the slope angle as the parameter of the environment that the model should deal with. Our work included simulations and experiments.

By the aid of the cell mapping method, the fixed points of the parameter combinations were determined. We have found that the increase of the moment of inertia has a positive effect on the step length and period, but a negative effect on the average speed. Enlarging the foot radius can increase all three descriptors; the only exception is the effect on the period when the k_J is very small. The effect of increasing the value of k_c is a bit complex. The step length and average speed decrease with the growth of k_c, but the speed does not decrease when the k_c is small. The periods along k_c show a decreasing–increasing shape when k_J is small, but when k_J increases, the inflection of the trend of the period is gradually postponed, and begins to show a steady decreasing trend. The basins of attraction of the fixed points are concerned with the sensitivity of the initial conditions of the models. A model with a large foot radius, small value of centre of mass and a large value of the moment of inertia has a large basin of attraction, and it can endure larger disturbance of initial conditions than ever reported before. We have designed uneven floors of random slope angle and random stairs to test the robustness of the model and used the fall ratio as a measure. A large foot radius and a small value of centre of

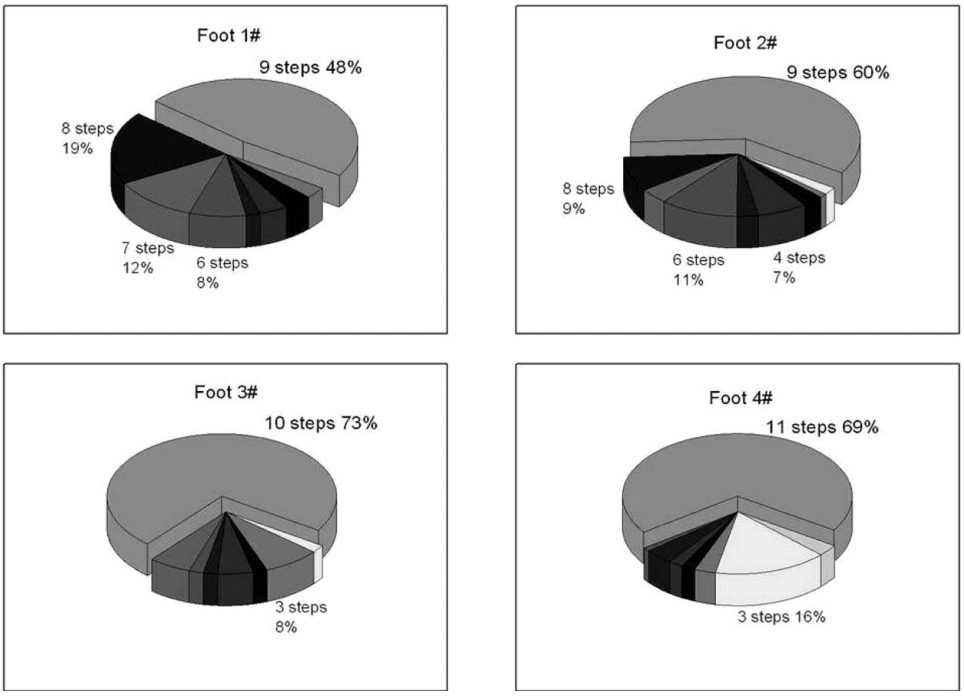

Fig. 20. Number of steps that the model with four types of feet could walk during 100 continuous manual releases.

https://doi.org/10.1017/S0263574708004906 Published online by Cambridge University Press

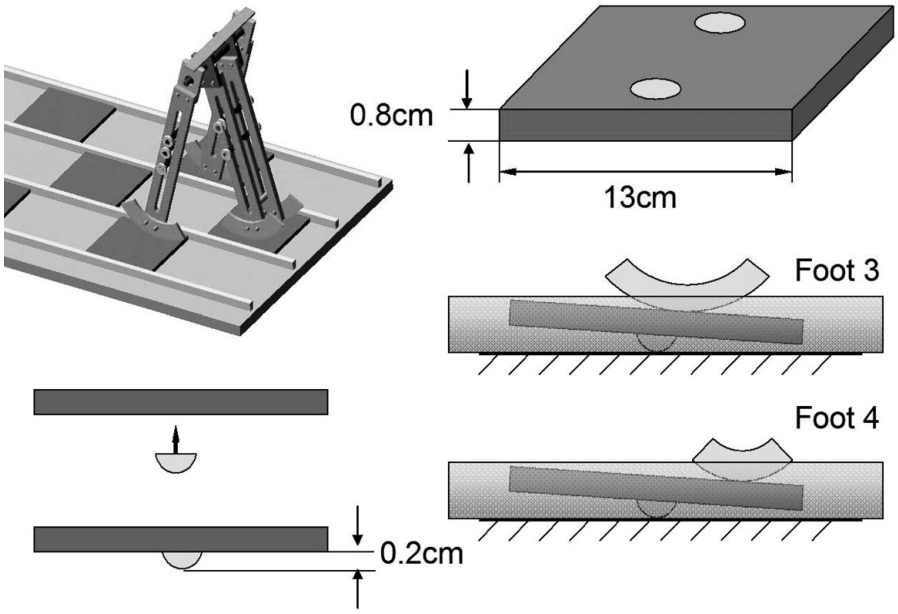

Fig. 22. Sketch map of the random angle floor.

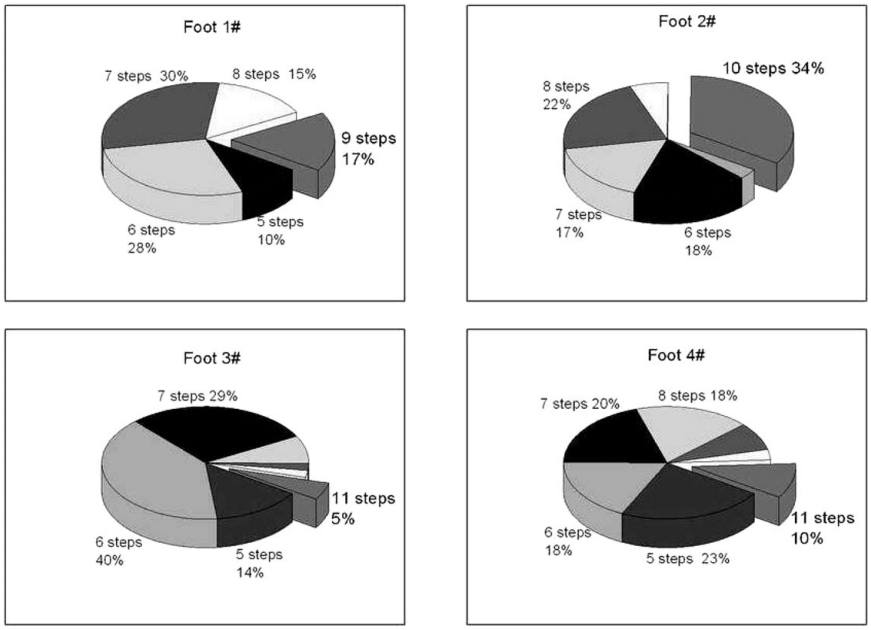

Fig. 23. Number of steps that the model with four types of feet could walk on the floor with random slope angles.

mass are needed for a robust model. A large moment of inertia is good for walking on floors with random slope angles, but a model with a small moment of inertia works well on floors with random stairs.

We have made a parameter-adjustable prototype to validate our simulation results. However, because of the model's structure, the centre of mass and the moment of inertia could not be adjusted in a large range, and thus we have only tested the prototype with different feet. During the experiments, the effects of increasing the foot radius on the step length, average speed and basin of attraction have been validated, and we think the exceptions were caused by the model asymmetry induced by the ground reaction force of the heelstrike. We designed a floor with approximate random slope angles to test the robustness of the model with different feet, and found that increasing the foot radius is also good for the robustness.

For the next step of simulation study, optimising the three parameters together to obtain a more robust pure passive model needs to be considered. We think such a model might be very significant for building an actuated model that can endure large disturbance. Limited by the configuration of the prototype, the moment of inertia and the centre of mass could not be adjusted in a wide range; thus, we only validated the simulation results related to the foot radius, and the remaining work will be finished using a new prototype.

References

1. T. McGeer, "Passive dynamic walking," *Int. J. Rob. Res.* **9**, 62–82 (Apr., 1990).

https://doi.org/10.1017/S0263574708004906 Published online by Cambridge University Press

2. S. Collins, M. Wisse and A. Ruina, "A three-dimensional passive-dynamic walking robot with two legs and knees," *Int. J. Rob. Res.* **20**, 607–615 (Jul. 2001).
3. M. Garcia, "Stability, Scaling, and Chaos in Passive Dynamic Gait Models," *Ph.D. Thesis* (Cornell University, 1999).
4. A. Goswami, B. Thuilot and B. Espiau, "A study of the passive gait of a compass-like biped robot: Symmetry and chaos," *Int. J. Rob. Res.* **17**, 1282–1301 (Dec. 1998).
5. A. D. Kuo, "Stabilization of lateral motion in passive dynamic walking," *Int. J. Robot. Res.* **18**, 917–930 (Sep. 1999).
6. J. Adolfsson, H. Dankowicz and A. Nordmark, "3D passive walkers: Finding periodic gaits in the presence of discontinuities," *Nonlin. Dyn.* **24**, 205–229 (2001).
7. S. Collins, A. Ruina, R. Tedrake and M. Wisse, "Efficient bipedal robots based on passive-dynamic walkers," *Science* **307**, 1082–1085 (2005).
8. M. Wisse, "Essentials of Dynamic Walking: Analysis and Design of Two-Legged Robots," *Ph.D. Thesis* (Delft University, 2005).
9. R. L. Tedrake, "Applied Optimal Control for Dynamically Stable Legged Locomotion," *Ph.D. Thesis* (MIT, 2004).
10. M. Garcia. A. Chatterjee, A. Ruina and M. J. Coleman, "The simplest walking model: Stability, complexity, and scaling," *ASME J. Biomech. Eng*. **120**, 281–288 (Apr. 1998).
11. M. Wisse, A. L. Schwab, R. Q. van der Linde and F. C. T. van der Helm, "How to keep from falling forward; elementary swing leg action for passive dynamic walkers," *IEEE Trans. Rob.* **21**, 393–401 (2005).
12. M. Wisse, A. L. Schwab and F. C. T. van der Helm, "Passive dynamic walking model with upper body," *Robotica* **22**(Part 6), 681–688 (2004).
13. M. Wisse, A. L. Schwab and R. Q. van der Linde, "A 3D passive dynamic biped with yaw and roll compensation," *Robotica* **19**(Part 3), 275–284 (2001).
14. A. Schwab and M. Wisse, "Basin of Attraction of the Simplest Walking Model," *Proceedings of International Conference on Noise and Vibration, ASME*, Pennsylvania (2001).
15. F. Asano and Z.-W. Luo, "On Energy-Efficient and High-Speed Dynamic Biped Locomotion with Semicircular Feet," *Proceedings of 2006 IEEE/RSJ International Conference on Intelligent Robots and Systems* (2006) pp. 5901–5906.
16. J. Hass, J. M. Herrmann and T. Geisel, "Optimal mass distribution for passivity-based bipedal robots," *Int. J. Rob. Res.* **25**, 1087–1098 (Nov. 2006).
17. Q. Wu and N. Sabet, "An experimental study of passive dynamic walking," *Robotica* **22**(Part 3), 251–262 (2004).
18. K. Byl and R. Tedrake, "Stability of Passive Dynamic Walking on Uneven Terrain," *Dynamic Walking 2006*, Ann Arbor, MI (2006).
19. J. L. Su and J. B. Dingwell, "Orbital Stability of Passive Dynamic Walking on a Bumpy Surface," *Proceedings of 30th Annual Meeting of the American Society of Biomechanics*, Blacksburg, VA (2006).
20. G. E. Daan Hobbelen and M. Wisse, "Limit Cycle Walking," **In**: *Humanoid Robots Human-like Machines* (Matthias Hackel, ed.) (I-Tech Education and Publishing, Vienna, Austria, 2007) pp. 277–294.
21. C. S. Hsu, *Cell-to-Cell Mapping: A Method of Global Analysis for Nonlinear Systems*. Applied Mathematical Sciences 64 (Springer, New York, 1987).
22. A. T. Safa, Mohammad Ghaffari Saadat and Mahyar Naraghi, "Passive dynamic of the simplest walking model: Replacing ramps with stairs" *Mech. Mach. Theory* **42**, 1314–1325 (2007).

https://doi.org/10.1017/S0263574708004906 Published online by Cambridge University Press